JPE 16-1-13

http://dx.doi.org/10.6113/JPE.2016.16.1.111
ISSN(Print): 1598-2092 / ISSN(Online): 2093-4718

A Novel IPT System Based on Dual Coupled Primary Tracks for High Power Applications

Yong Li[*,**], Ruikun Mai[*,†], Liwen Lu[*,**], and Zhengyou He[*,**]

[*]Key Laboratory of Magnetic Suspension Technology and Maglev Vehicle, Ministry of Education, Chengdu, China
[**,†]Department of Electronic Engineering, Southwest Jiaotong University, Chengdu, China

Abstract

Generally, a single phase H-bridge converter feeding a single primary track is employed in conventional inductive power transfer systems. However, these systems may not be suitable for some high power applications due to the constraints of the semiconductor switches and the cost. To resolve this problem, a novel dual coupled primary tracks IPT system consisting of two high frequency resonant inverters feeding the tracks is presented in this paper. The primary tracks are wound around an E-shape ferrite core in parallel which enhances the magnetic flux around the tracks. The mutual inductance of the coupled tracks is utilized to achieve adjustable power sharing between the inverters by configuring the additional resonant capacitors. The total transfer power can be continuously regulated by altering the pulse width of the inverters' output voltage with the phase shift control approach. In addition, the system's efficiency and the control strategy are provided to analyze the characteristic of the proposed IPT system. An experimental setup with total power of 1.4kW is employed to verify the proposed system under power ratios of 1:1 and 1:2 with a transfer efficiency up to 88.7%. The results verify the performance of the proposed system.

Key words: Dual primary tracks, Inductive Power Transfer (IPT), Power distribution, Power sharing

I. INTRODUCTION

Inductive Power Transfer (IPT) is a promising way to deliver power from a power source to a load or multiple loads via electromagnetic coupling in order to enhance system flexibility [1]-[17]. Nowadays, IPT systems have been employed in numerous applications which include low power wireless charging of biomedical implants [10], electric vehicle charging systems [16], and public transport systems [17].

Only one primary track with an elongate loop or a pad is supplied by a single resonant inverter in conventional IPT systems, and an IPT pick-up consists of a coil of litz wire in close proximity to the track wires positioned to capture magnetic flux around the track conductor as shown in Fig. 1. The magnitude and frequency of the track current, and the magnetic coupling and quality factor of the compensated circuit directly dictate the amount of power that can be transferred across the air gap. As a result, high voltage, high current, high frequency semiconductor devices are used to achieve a high power transfer. However, these semiconductor devices are relatively expensive and may not be easy to purchase.

Multilevel technology [18]-[20] has advantages in terms of reducing the stress of semiconductor devices, and in implementing high power IPT systems by using low-cost and low-voltage semiconductor devices. However, it is a challenge to implement such systems at high frequency and to get them to work under the soft switch condition. Multi-inverter connected in parallel is another option to realize high power transfer by using low power capacity resonant inverters. A parallel topology for IPT systems by connecting identical LCL-T-based IPT supplies in parallel across a shared ac track inductor was proposed in [8]. This topology can dramatically improve the system's transfer power, availability and reliability. However, large circulating currents among the inverter modules may be generated by the component tolerance, and the control strategy used to minimize the circulating currents is complex.

Multi-coil connected with multi-inverter is employed in induction heating to enhance the magnetic fields, which can

Manuscript received May 21, 2015; accepted Aug. 28, 2015
Recommended for publication by Associate Editor Chun-An Cheng.
[†]Corresponding Author: mairk@swjtu.cn
Tel: +86-028-87602445, Southwest Jiaotong University
[*]Key Laboratory of Magnetic Suspension Technology and Maglev Vehicle, Ministry of Education, China
[**]Dept. of Electronic Eng., Southwest Jiaotong University, China

© 2016 KIPE

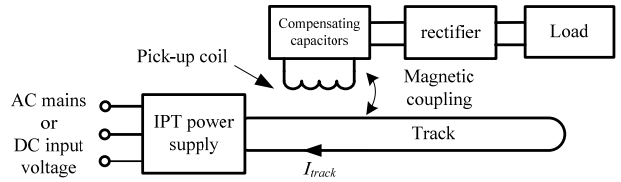

Fig. 1. Typical IPT system.

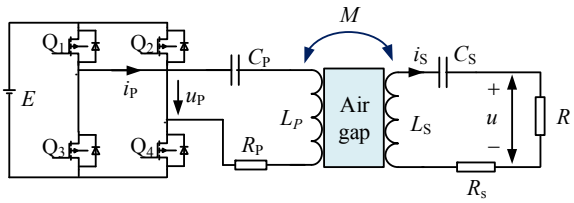

Fig. 2. The structure of the IPT system based on single track.

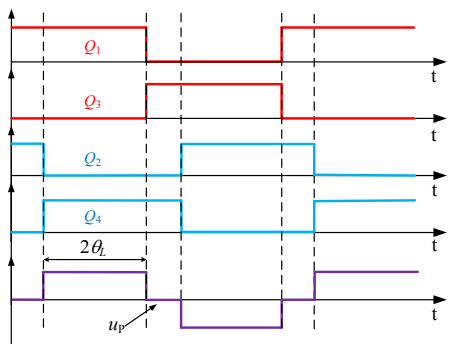

Fig. 3. Principal operation waveforms of inverter.

enhance the total output power by using multiple low power inverters [21]-[26]. On the one hand, the limitations of its single operation can be removed in aspects like heat dissipation, cost, short time overload, and component limitations. On the other hand, the multi-coils connected with multi-inverter also brings convenience in terms of maintenance and flexible operation for maximum efficiency and reliability. However, the mutual inductances among the coils makes it difficult to control the resonant currents flowing through the coils. An additional decoupling transformer is one of the solution to mitigate the influence of mutual inductances [25]-[26]. However, this comes with an increase in cost.

This paper presents a new IPT topology based on dual coupled tracks connected to double resonant inverters to meet the demand of high-power applications. The mutual inductance of the dual coupled tracks is utilized to achieve better power sharing between the inverters or to improve the power distribution by configuring the resonant capacitor. Resonant inverters with different power capacities can be chosen to achieve maximum power transfer by altering the additional capacitors with a careful design. An experimental setup with a total transfer power of 1.4kW is employed to verify the proposed system under power ratios of 1:1 and 1:2 between the two inverters with an approximate transfer efficiency of 88.5%. According to the results, an attractive option for integrating low-power inverters of identical or different power capacities with dual coupled tracks is built to meet the demands of high-power applications.

The rest of this paper is organized as follows. A review of IPT systems based on a single track is shown in In Section II. In Section Ⅲ, a detailed description of the structure design and principle analysis of an IPT system based on dual coupled tracks connected with double resonant inverters is given; and the parameter design and power distribution method for the proposed IPT system is analyzed in detail. Then, Section Ⅳ shows steady-state results of an experimental system operating at 1.4kW. Some conclusions are then given in Section V.

II. Review of IPT Systems Based on a Single Track

A conventional IPT system based on a single primary track is shown in Fig. 2. It comprises a high frequency H-bridge resonant inverter, a full-bridge rectifier, and resonant tanks. L_P and L_S are the inductances of the primary track and the pick-up coil, respectively. C_P and C_S are the resonant capacitors used to compensate the primary track L_P and the pick-up L_S. The equivalent series resistances of the track and the pick-up coil are R_1 and R_S, which can be neglected since their values are relatively small compared to that of the load. The mutual inductances between the pick-up coil and the primary tracks are denoted as M.

The inverter is controlled by the phase-shift technique, which generates a fixed-frequency ac output voltage u_P as shown in Fig. 3. The operating frequency of the inverter is equal to the resonant frequency $\omega = \frac{1}{\sqrt{L_P C_P}} = \frac{1}{\sqrt{L_S C_S}}$.

According to [5], the RMS (Root Mean Square) of the track current can be obtained as:

$$I_P = \frac{2\sqrt{2}ER\sin(\theta_L)}{\omega^2 M^2 \pi} \quad (1)$$

According to [5], the transfer power can be calculated by:

$$P_t = \frac{(I_P \omega M)^2}{R} \quad (2)$$

Therefore, the transfer power of IPT systems can be upgraded by enhancing the equivalent track current.

III. Analysis and Design of IPT Systems Based on Dual Coupled Tracks

A. Description of the Proposed IPT System

An IPT system based on dual coupled tracks is shown in Fig. 4. The dual tracks are wound in parallel around an E-shaped ferrite core over several-tens of meters as a power transmitter, and each track is connected with an H-bridge resonant inverter

as a power supply converter. In addition, all of the inverters share a common DC input voltage. A pick-up coil is wound around an E-shaped ferrite core as a power receiver. The power receiver is intentionally shorter than the power transmitter, so that it can dynamically move over the primary tracks freely.

In order to analyze the magnetic field of the proposed structure, a commercial finite-element analysis software, i.e., Flux is employed to provide the magnetic field image shown in Fig. 5. This is done with an energized current of 10A for a single track, 5A each for dual tracks, and 10A each for dual tracks. It is clear that the magnetic field intensity of 10A for a single track is very close to that of one 5A for each of the dual tracks due to the parallel structure. The magnetic field is dynamically strengthened by increasing the current to 10A each for the dual tracks as the equivalent current increases. In other words, the total magnetic field around the power transmitter is synthesized by the dual tracks' currents. As a result, the transfer power is enhanced by the synthesized magnetic field, which is energized by the two currents. Under this condition, a relatively large mutual inductance M_{12} exists between the coupled primary tracks. This large mutual inductance is utilized to obtain better power sharing performance of the IPT system instead of decoupling the inductor behavior to simplify the system as done in classical approaches [25], [26].

The equivalent circuit of an IPT system with the series-series tuned topology is depicted in Fig. 6. L_1, L_2 and L_S are the inductances of the primary track 1, track 2 and the pick-up coil, respectively. C_1, C_2 and C_S are the resonant capacitors used to compensate the primary tracks L_1 and L_2, and the pick-up coil L_S. The equivalent series resistances of the dual tracks and the pick-up coil are R_1, R_2, and R_S. The mutual inductances between the pick-up coil and the primary dual tracks are M_{1S} and M_{2S}, respectively. A full bridge rectifier is employed to convert high frequency AC power to DC power to feed the load R_L. The two-inverter units operate at an identical angular frequency of ω, which can be defined by:

$$\omega = \frac{1}{\sqrt{L_1 C_1}} = \frac{1}{\sqrt{L_2 C_2}} = \frac{1}{\sqrt{L_S C_S}} \tag{3}$$

For simplicity of analysis and design, the structure of the dual primary tracks are designed identically. In addition, both of the mutual inductances between the pick-up coil and the primary dual tracks are approximately identical, M_{1S}=M_{2S}.

The inverters are controlled by the phase-shift technique, which generates fixed-frequency ac output voltages u_1 and u_2. Moreover, the voltages are identical to each other by employing synchronous control technology [8], as shown in Fig. 7.

The fundamental voltage phasor of the inverters can be derived as:

$$\dot{U}_1 = \dot{U}_2 = \frac{2\sqrt{2}E\sin(\theta_L)}{\pi} \tag{4}$$

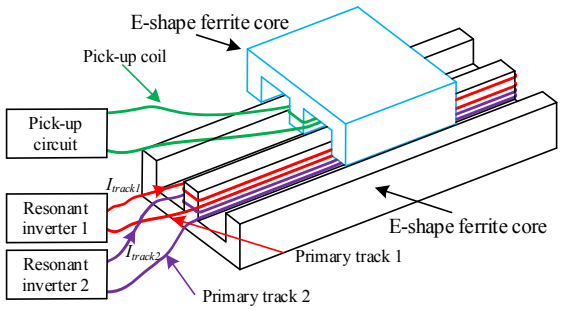

Fig. 4. The structure of the proposed IPT system.

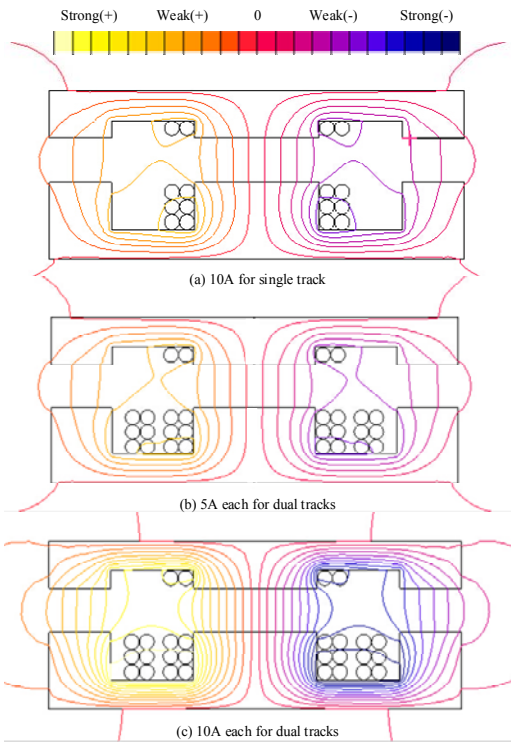

Fig. 5. Magnetic field image of the single track and dual tracks structure with different energized currents.

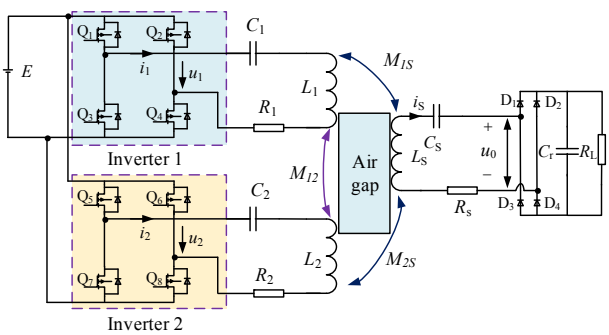

Fig. 6. The equivalent circuit of the proposed series-series tuned IPT system.

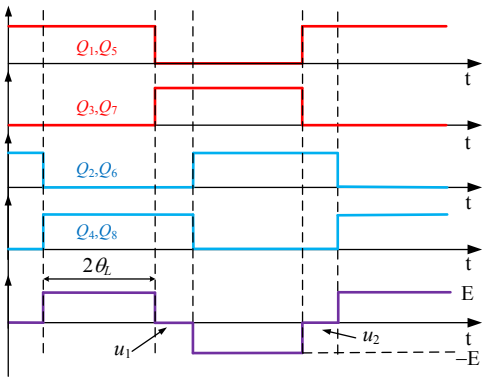

Fig. 7. Principal operation waveforms of inverter 1 and inverter 2.

B. Modeling and Analysis of the Proposed IPT System

According to mutual coupling theories, the relationship between the current values and the voltages can be derived as:

$$\begin{bmatrix} \dot{U}_1 \\ \dot{U}_2 \\ 0 \end{bmatrix} = \begin{bmatrix} Z_1 & j\omega M_{12} & j\omega M_{1S} \\ j\omega M_{12} & Z_2 & j\omega M_{2S} \\ j\omega M_{1S} & j\omega M_{2S} & Z_S \end{bmatrix} \begin{bmatrix} \dot{I}_1 \\ \dot{I}_2 \\ \dot{I}_S \end{bmatrix} \tag{5}$$

where Z_1, Z_2 and Z_S are the impedances of the dual primary tracks and the pick-up, respectively. The impedances can be defined as follow:

$$\begin{bmatrix} Z_1 \\ Z_2 \\ Z_S \end{bmatrix} = j\omega \begin{bmatrix} L_1 \\ L_2 \\ L_S \end{bmatrix} + \frac{1}{j\omega} \begin{bmatrix} 1/C_1 \\ 1/C_2 \\ 1/C_S \end{bmatrix} + \begin{bmatrix} R_1 \\ R_2 \\ R_S + R_0 \end{bmatrix} \tag{6}$$

For simplicity of the analysis, the equivalent series resistances of the dual tracks and the pick-up coil are neglected since their values are relatively small compared to that of the load. That this is to say, R_S=R_1=R_2=0, Z=Z_1=Z_2=0, and Z_S = R_0.

According to [27], the equivalent load R_0 of the rectified tank connected to a resistive load R_L can be expressed by:

$$R_0 = \frac{8R_L}{\pi^2} \tag{7}$$

By substituting (4), (6), and (7) into (5), the fundamental current phasor of the dual tracks can be derived by:

$$\dot{I}_1 = \dot{I}_2 = \frac{8\sqrt{2}E\sin(\theta_L)R_L(\omega\pi^2 M_{1S}^2 - j4R_L M_{12})}{\pi^3\omega(\pi^2\omega^2 M_{1S}^4 + 2R_L {M_{12}}^2)} \tag{8}$$

The impedances of the H-bridge inverter units can be yielded by:

$$\begin{bmatrix} Z_1 \\ Z_2 \end{bmatrix} = \begin{bmatrix} \dfrac{\dot{U}_1}{\dot{I}_1} \\ \dfrac{\dot{U}_2}{\dot{I}_2} \end{bmatrix} = \begin{bmatrix} \dfrac{\pi^2\omega^2}{4R_L} & j\omega \\ \dfrac{\pi^2\omega^2}{4R_L} & j\omega \end{bmatrix} \begin{bmatrix} M_{1S}^2 \\ M_{12} \end{bmatrix} \tag{9}$$

Under this condition, the H-bridge inverter units' impedances are not purely resistive due to the mutual inductance between the dual tracks. Therefore, the inverter units are not working under the resonant condition. That is to say, the capacitors are used to compensate the primary track since the traditional method do cannot meet the requirements of the resonance in dual coupled tracks IPT systems.

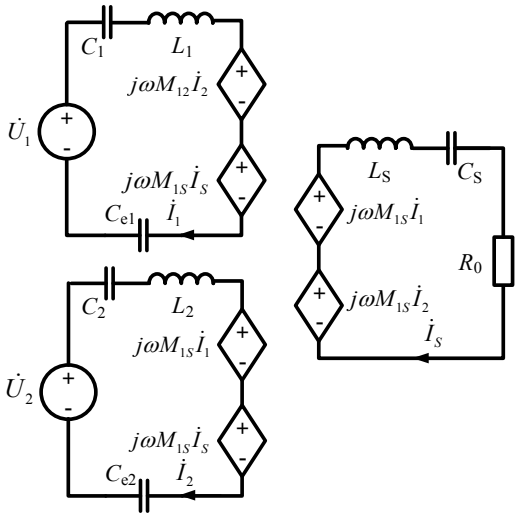

Fig. 8. The equivalent circuit diagram with additional compensation capacitors.

C. Parameter Design and Power Distribution

According to the aforementioned analysis, in order to minimize the reactive power of the H-bridge inverters, additional capacitors C_{e1} and C_{e2} are added to ensure that the H-bridge inverters to work under the resonance condition. An equivalent circuit diagram with the additional capacitors is shown in Fig. 8.

Assuming that $jX_1 = (j\omega C_{e1})^{-1}$ and $jX_2 = (j\omega C_{e2})^{-1}$, according to (6), the impedance of the dual primary tracks can be derived by:

$$\begin{aligned} \begin{bmatrix} Z_1' \\ Z_2' \end{bmatrix} &= j\omega \begin{bmatrix} L_1 \\ L_2 \end{bmatrix} + \frac{1}{j\omega} \begin{bmatrix} 1/C_1 \\ 1/C_2 \end{bmatrix} + \frac{1}{j\omega} \begin{bmatrix} 1/C_{e1} \\ 1/C_{e2} \end{bmatrix} + \begin{bmatrix} R_1 \\ R_2 \end{bmatrix} \\ &= \begin{bmatrix} jX_1 \\ jX_2 \end{bmatrix} \end{aligned} \tag{10}$$

For the sake of convenience, the following variables in (11) are defined:

$$\begin{cases} A = \omega^2\pi^2 M_{1S}(X_1 + X_2 - 2\omega M_{12}) \\ B = (X_1 X_2 - \omega^2 {M_{12}}^2) \end{cases} \tag{11}$$

Under these conditions, substituting (4), (7), and (10) into (5), the fundamental current phasor of the dual tracks can be changed to:

$$\begin{bmatrix} \dot{I}_1' \\ \dot{I}_2' \end{bmatrix} = \frac{j16\sqrt{2}ER_L\sin(\theta_L)}{\pi\left[8R_L(\omega^2 {M_{1S}}^2 - X_1X_2) + jA\right]} \begin{bmatrix} X_2 - \omega M_{12} \\ X_1 - \omega M_{12} \end{bmatrix} \tag{12}$$

The new impedances of the H-bridge inverter units can be yielded by:

$$\begin{bmatrix} Z_1' \\ Z_2' \end{bmatrix} = A \begin{bmatrix} \dfrac{1}{8X_2R_L - 8\omega R_L M_{12}} \\ \dfrac{1}{8X_1R_L - 8\omega R_L M_{12}} \end{bmatrix} + jB \begin{bmatrix} \dfrac{1}{X_2 - \omega M_{12}} \\ \dfrac{1}{X_1 - \omega M_{12}} \end{bmatrix} \quad (13)$$

In order to let the two H-bridge inverter work under the resonant condition, the H-bridge inverter units' impedance has to be purely resistive. Meanwhile, to make the two inverter output power levels flexibly configured, $\mathrm{Re}(Z_1')$ is set to be equal to $\lambda \mathrm{Re}(Z_2')$. $\mathrm{Re}(\bullet)$ represents the real component operation for $(\bullet)$. That is to say, the output power of inverter 2 is λ times that of inverter 1. Consequently, it is possible to obtain:

$$\begin{cases} B = 0 \\ \dfrac{A}{8X_2R_L - 8\omega R_L M_{12}} = \lambda \cdot \dfrac{A}{8X_1R_L - 8\omega R_L M_{12}} \end{cases} \quad (14)$$

The solution of (14) is given by

$$\begin{bmatrix} X_1 \\ X_2 \end{bmatrix} = -\omega M_{12} \begin{bmatrix} \lambda \\ 1/\lambda \end{bmatrix} \quad (15)$$

The value of the additional capacitors can be derived by:

$$\begin{bmatrix} C_{e1} \\ C_{e2} \end{bmatrix} = \frac{1}{\omega^2 M_{12}} \begin{bmatrix} 1/\lambda \\ \lambda \end{bmatrix} \quad (16)$$

Therefore, by adding the additional capacitors C_{e1} and C_{e2}, the impedances of the H-bridge inverter units are purely resistive as shown below:

$$\begin{bmatrix} Z_1'' \\ Z_2'' \end{bmatrix} = \frac{\pi^2 \omega^2 {M_{1S}}^2 (\lambda+1)}{8R_L} \begin{bmatrix} 1 \\ 1/\lambda \end{bmatrix} \quad (17)$$

The relationship between the dual tracks' currents can be expressed by:

$$\dot{I}_2'' = \lambda \dot{I}_1'' = \frac{\lambda}{(\lambda+1)} \cdot \frac{16\sqrt{2}ER_L \sin(\theta_L)}{\pi^3 \omega^2 {M_{1S}}^2} \quad (18)$$

The output power of each inverter can be derived by:

$$\begin{bmatrix} P_1 \\ P_2 \end{bmatrix} = \begin{bmatrix} \mathrm{Re}[\dot{U}_1 \cdot (\dot{I}_1'')^*] \\ \mathrm{Re}[\dot{U}_2 \cdot (\dot{I}_2'')^*] \end{bmatrix} = \frac{64E^2 R_L \sin^2(\theta_L)}{\pi^4 \omega^2 M_{1S}^2 (\lambda+1)} \begin{bmatrix} 1 \\ \lambda \end{bmatrix} \quad (19)$$

where $(\bullet)^*$ represents the conjugate operation for $(\bullet)$. The total output power (P) of the primary side can be given by:

$$P = P_1 + P_2 = \frac{64E^2 R_L \sin^2(\theta_L)}{\pi^4 \omega^2 M_{1S}^2} \quad (20)$$

All in all, the mutual inductance between the dual tracks is compensated by using the additional capacitors, which ensures that the inverters can work under the resonance condition. The inverters' output power can be effectively allocated by choosing an appropriate value of λ. Moreover, no matter what the value λ is, the total output power of the inverters remains the same.

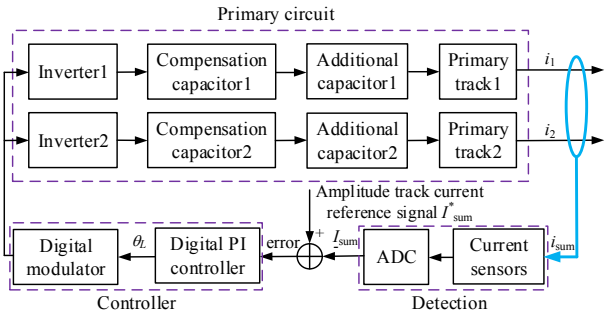

Fig. 9. Current control diagram.

According to the aforementioned analysis, the voltage ratings of the semiconductor of a conventional IPT system and that of the proposed IPT system are decided by the DC input voltage E. The operating frequency of a conventional IPT system is identical to that of the proposed IPT system with the resonant frequency. Therefore, both the voltage rating and frequency of the semiconductor used for conventional IPT systems and the proposed IPT system are the same.

As can be seen from (1), (7), and (18), if M=M_{1S} and $R = R_0$, it is possible to obtain:

$$\begin{bmatrix} I_1 \\ I_2 \end{bmatrix} = \begin{bmatrix} 1 \\ \lambda \end{bmatrix} \frac{I_P}{(\lambda+1)} = \begin{bmatrix} 1 \\ \lambda \end{bmatrix} \frac{2\sqrt{2}ER\sin(\theta)}{\omega^2 M^2 \pi(\lambda+1)} \quad (21)$$

Therefore, the current ratings of the semiconductor for the proposed IPT system are $1/(\lambda+1)$ or $\lambda/(\lambda+1)$ times the current ratings of the semiconductor for a conventional IPT system.

D. Track Current Control

In order to simplify the pickup control, it is necessary to regulate the track current at a designed value since the received voltage by a pickup is directly proportional to the track current.

A simplified view of the control loop is illustrated in Fig. 9. The controller controls and regulates the amplitude of the total track current i_{sum} (i_1+i_2) by varying the inverter conduction angle θ_L shown in Fig. 7, which is the input to the current control loop. The primary objective of the controller is to improve the reference tracking performance of the power supply.

IV. System Efficiency

To analyze the system efficiency, the resistances R_S, R_1, and R_2 in Fig. 4 should be considered. Assume that the equivalent series resistances are equal (R_1=R_2) because the

structure of the dual primary tracks are arbitrarily designed identically. $\lambda = 1$ is widely used to achieve better power sharing when the H-bridge inverters have identical power capacities. In order to simplify the analysis, the system efficiency is analyzed in detail considering only $\lambda = 1$. The impedance of the dual primary circuits can be derived by:

$$Z_{p1}=Z_{p2}=\frac{2\omega^2 {M_{1S}}^2}{R_0+R_S}+R_1 \tag{22}$$

The output power of inverter 1 and inverter 2 can be expressed by:

$$\begin{bmatrix} P_1 \\ P_2 \end{bmatrix}=\begin{bmatrix} \frac{\dot{U}_1\left(\dot{U}_1\right)^*}{Z_{p1}} \\ \frac{\dot{U}_2\left(\dot{U}_2\right)^*}{Z_{p2}} \end{bmatrix}=\begin{bmatrix} \frac{\left|\dot{U}_1\right|^2\left(R_0+R_S\right)}{2\omega^2 {M_{1S}}^2+R_0R_1+R_SR_1} \\ \frac{\left|\dot{U}_2\right|^2\left(R_0+R_S\right)}{2\omega^2 {M_{1S}}^2+R_0R_1+R_SR_1} \end{bmatrix} \tag{23}$$

The voltage phasor of the pick-up coil can be derived by:

$$\begin{aligned} \dot{U}_S &= j\left(\dot{I}_1+\dot{I}_2\right)\omega M_{1S}=j\left(\frac{\dot{U}_1}{Z_{p1}}+\frac{\dot{U}_2}{Z_{p2}}\right)\omega M_{1S} \\ &=\frac{j2\omega M_{1S}\left|\dot{U}_1\right|^2\left(R_0+R_S\right)}{\omega^2 {M_{1S}}^2+R_0R_1+R_SR_1+\omega^2 {M_{1S}}^2} \end{aligned} \tag{24}$$

The current phasor of the secondary circuit is given by:

$$\dot{I}_S=\frac{\dot{U}_S}{R_0+R_S}=\frac{j2\dot{U}_1\omega M_{1S}}{2\omega^2 {M_{1S}}^2+R_0R_1+R_SR_1} \tag{25}$$

The output power of the IPT system is derived by:

$$\begin{aligned} P_o &= \dot{I}_S\left(\dot{I}_S\right)^* R_0 \\ &=\left(\frac{2\left|\dot{U}_1\right|\omega M_{1S}}{2\omega^2 {M_{1S}}^2+R_0R_1+R_SR_1}\right)^2 R_0 \end{aligned} \tag{26}$$

Therefore, the efficiency of the IPT system can be derived by:

$$\eta=\frac{P_0}{P_1+P_2}=\frac{2\omega^2 R_0 {M_{1S}}^2}{(R_0+R_S)(2\omega^2 {M_{1S}}^2+R_0R_1+R_SR_1)} \tag{27}$$

To achieve maximum efficiency, the equivalent series resistances of the dual tracks and the pick-up coil R_S, R_1, and R_2 should be designed as small as possible.

In order to calculated the maximum efficiency of the IPT system, the derivation of η should be set to zero.

$$\frac{d\eta}{dR_0}=0 \tag{28}$$

The theoretical optimal load R_0 corresponding to the maximum efficiency can be obtained as:

$$R_0=\frac{\sqrt{R_S}\sqrt{2{M_{1S}}^2\omega^2+R_1R_S}}{\sqrt{R_1}} \tag{29}$$

Under this optimal load, the maximum efficiency can be obtained as:

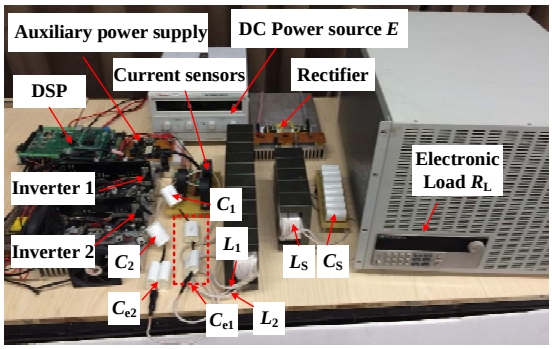

Fig. 10. The exterior appearance of the proposed IPT prototype.

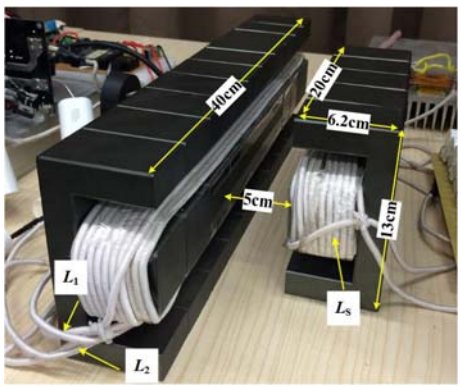

Fig. 11. The tracks and the pick-up coil wound around ferrite core with Litz wire.

$$\eta_{\max}=\frac{{M_{1S}}^2\omega^2\sqrt{2{M_{1S}}^2\omega^2+R_1R_S}}{(R_1R_S)^{3/2}+\left(\omega^2 {M_{1S}}^2+R_1R_S\right)\sqrt{2{M_{1S}}^2\omega^2+R_1R_S}+2{M_{1S}}^2\omega^2\sqrt{R_1R_S}} \tag{30}$$

By choosing an optimal load, maximum efficiency can be achieved.

V. Experimental Verification

A. Prototype System

To validate the proposed topology and power distribution method, an experimental IPT prototype was constructed in a laboratory settings with dual primary tracks connected to dual H-bridge inverters as shown in Fig. 4. The prototype was designed to operate up to 20 kHz and 1.4kW in the experiment. It can implement the power distribution method by choosing proper additional capacitors.

The exterior appearance of the experimental setup is portrayed in Fig. 10. Two inverters are separately powered by a common DC supply, and the AC output of the two H-bridge inverters are connected to the tracks.

The gate pulse signals for the active switches are generated by a TMS320F28335 Digital Signal Processor (DSP, Texas Instrument). A CONCEPT-2SC0108T2A0-17 is adopted as the power MOSFET drive to fulfill the requirements of a high switching frequency.

The dual tracks are wound with Litz wire around an E type ferrite core, and the pick-up coil is also wound around an E

TABLE I
THE CONFIGURATION OF THE IPT SYSTEM

Parameters	Value
DC voltage of the H-bridge inverters unit E/V	70
Inverter frequency f/kHz	20
Inductance of the track 1 $L_1 / \mu H$	63
Inductance of the track 2 $L_2 / \mu H$	63
Resonant compensation capacitance of track 1 $C_1 / \mu F$	1.0
Resonant compensation capacitance of track 2 $C_2 / \mu F$	1.0
Mutual inductance between the tracks $M_{12} / \mu H$	60.73
Mutual inductance of the tracks and pick-up coil $M_{1S} / \mu H$	24.5
Inductance of the pick-up coil $L_S / \mu H$	36.2
Resonant compensation capacitance of pick-up circuit $C_S / \mu F$	1.749
Equivalent resistance of the load R_L / Ω	3.5

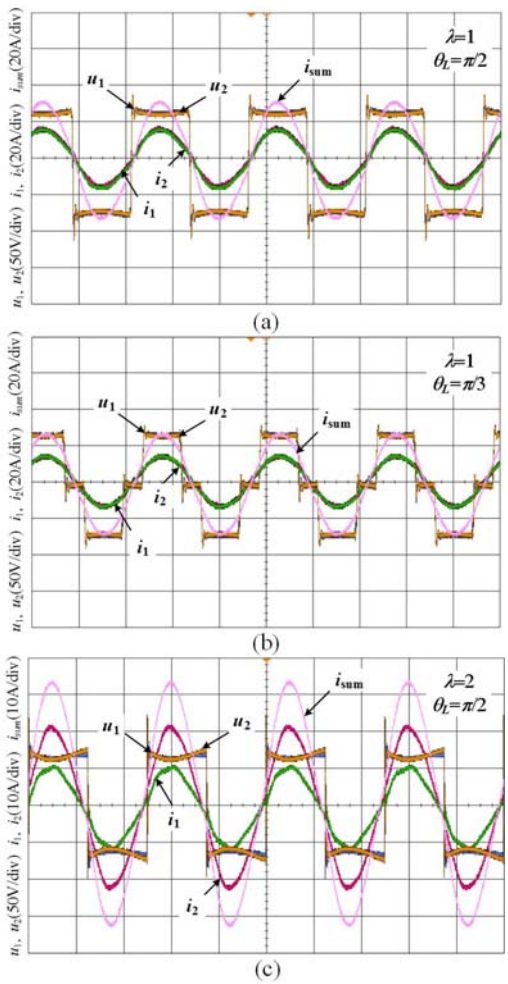

Fig. 12. Output currents and voltages of the inverters: (a) $\lambda = 1$ and $\theta_L = \pi/2$, (b) $\lambda = 1$ and $\theta_L = \pi/3$, and (c) $\lambda = 2$ and $\theta_L = \pi/2$.

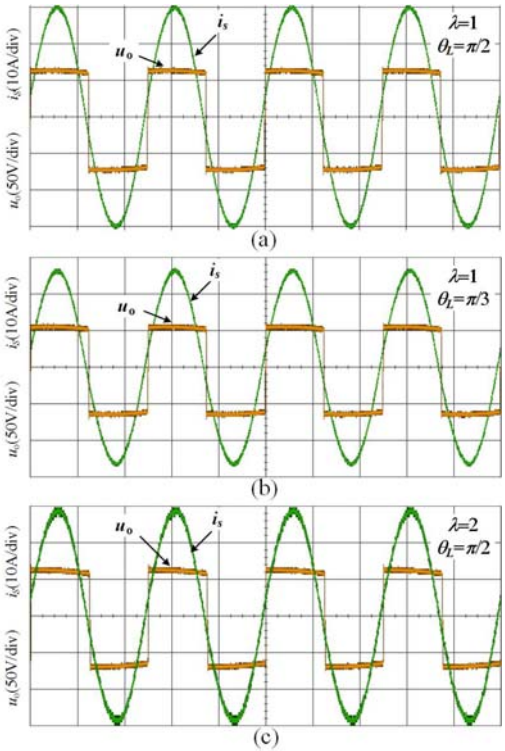

Fig. 13. Pick-up output current and voltage: (a) $\lambda = 1$ and $\theta_L = \pi/2$, (b) $\lambda = 1$ and $\theta_L = \pi/3$, and (c) $\lambda = 2$ and $\theta_L = \pi/2$.

type ferrite core with Litz wire. The ferrite core sizes are shown in Fig. 11. The air gap between the tracks and the secondary pick-up coil is set to be 5cm.

The mutual and track inductances were measured by an Agilent E4980A LCR meter. Moreover, an oscilloscope Agilent MSO-X 4034A was used to measure and display the current and voltage waveforms of interest by means of N2780B current probes and N2891A differential probes, respectively.

The design specifications of the prototype and the experimental setup are listed in TABLE I.

B. Experimental Results

Without a loss of generality, two settings ($\lambda = 1$ and $\lambda = 2$) are performed to validate the performance of the proposed algorithm. The additional compensation capacitors are calculated as C_{e1}=C_{e2}=1.04μF and C_{e1}=4C_{e2}=0.52μF according to (16). Under these conditions, a number of experimental results have been tested by altering θ_L. However, only three sets of experimental waveforms are provided in Fig. 12 and Fig. 13 due to limitation on the paper's length.

The output currents i_1, i_2 and voltages u_1, u_2 of the two H-bridge inverters are illustrated in Fig. 12 for the corresponding measured waveforms. i_{sum} is the sum of the two inverter currents i_1 and i_2. In Fig. 12 (a) and (b), show

TABLE II
PERFORMANCE OF PROPOSED IPT SYSTEM UNDER VARIOUS CONDITIONS

Case	λ	θ_L (rad)	P_1 (W)	P_2 (W)	P_0 (W)	η (%)
A	1	$\pi/2$	706.91	703.87	1253.2	88.7
B	1	$\pi/3$	528.07	527.46	890.03	84.0
C	2	$\pi/2$	470.26	939.47	1249.0	88.6

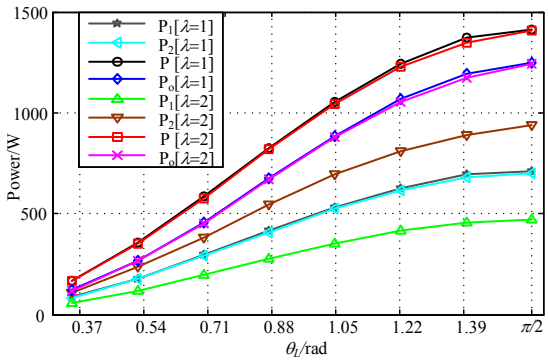

Fig. 14. Relation between the output power of the inverters and θ_L .

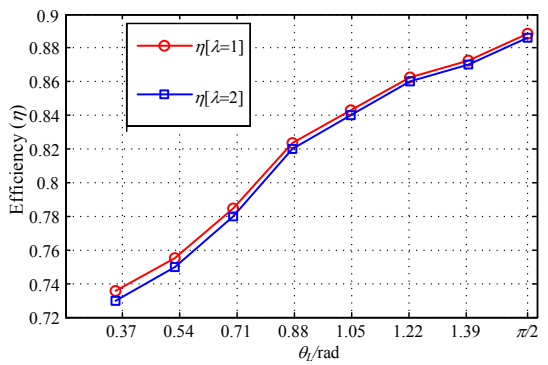

Fig. 15. Relation between the efficiency and θ_L .

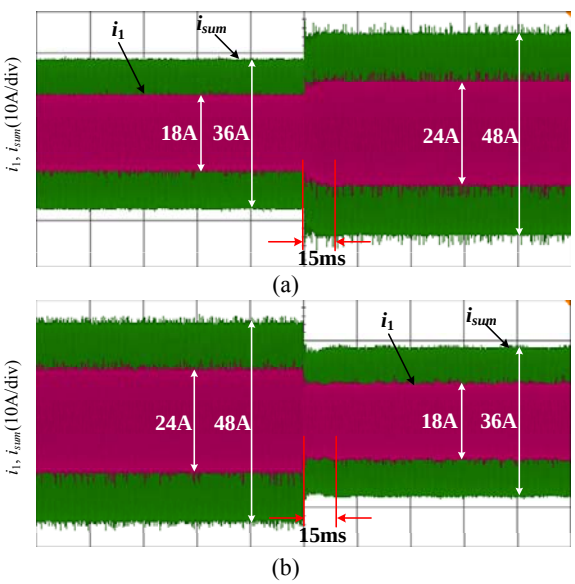

Fig. 16. Closed loop system response to step change in reference track current: (a) From 18A to 24 A and (b) From 24A to 18A.

that the currents of the two inverters are identical when $\lambda = 1$ with $\theta_L = \pi/2$ and $\theta_L = \pi/3$. In this case, the output current of one inverter is not only in phase with that of the other, but also in phase with the output voltage. This shows that both of the inverters are working under the resonance condition. When $\lambda = 2$, the current of the first inverter is in phase with the other but with twice the magnitude as shown in Fig. 12(c). The voltage and current waveforms of the load are illustrated in Fig. 13 and the measured powers (P_1 and P_2 are the output power of inverter 1 and inverter 2, and P_o is the load consumption power) are listed in TABLE II

The output power of Case A is approximately the same as that of Case C. The output power of both of the inverters in Case A are nearly identical, while the output power of one inverter in Case C is nearly twice as that of the other. This means the power sharing of the two inverters can be achieved by the proposed method. The output power and the system's efficiency decrease as θ_L goes down for both cases, as shown in Fig. 15.

To provide a clear comparison of the different operating conditions, the experimental values of the output powers of each inverter and total output power against θ_L are given in Fig. 14. The experimental results clearly show that wide-range output power regulation can be attained by altering θ_L, and that power sharing can be achieved by the proposed method.

The dynamic current response with $\lambda = 1$ is shown in Fig. 16 with two test cases. One is for changing the reference amplitude value of the current i_{sum} from 18A to 24A and the other is for changing it from 24A to 18A. The blue line is the summation of the total track current i_{sum}, and the red line is the first track current i_1. It needs only 15ms to settle down to the reference current for both cases, which shows the good performance of the dynamic response. In addition, i_1 is half of i_{sum} for both cases.

In conclusion, according to the aforementioned experimental results, the power distribution of the two inverters can be allocated by adopting different values of λ, which validates the proposed power distribution and control methods.

VI. CONCLUSION

A novel IPT system based on dual coupled primary tracks is proposed in this paper. The structure of an IPT system has been explained and described in detail. In addition, the magnetic, system's efficiency and the control strategy are provided to analyze the characteristic of the proposed IPT system. The mutual inductance of the dual coupled tracks is utilized to achieve better power sharing between the inverters or to improve the power distribution by configuring additional capacitors. Furthermore, both of the inverters can work under resonance conditions. The output power can be continuously

regulated by altering the output voltage pulse width of the inverters. A 1.4kW experimental prototype is set up and tested to verify power ratios of 1:1 and 1:2 with a transfer efficiency up to 88.7%. The experimental results verify the performance of the proposed IPT system and the power distribution approach, which is suitable for high power IPT applications with various power level requirements.

ACKNOWLEDGMENT

This work was supported by Scientific R&D Program of China Railway Corporation (2014J013-B) and National Natural Science Foundation of China (Grant No. 51507147) and the Fundamental Research Funds for the Central Universities (2682015CX021).

REFERENCES

[1] X. Dai, Y. Zou, and Y. Sun, "Uncertainty Modeling and Robust Control for LCL Resonant Inductive Power Transfer System," *Journal of Power Electronics*, Vol. 13, No. 5 pp. 814-828, Sep. 2013.

[2] Y. L. Li, Y. Sun, and X. Dai, "μ-Synthesis for Frequency Uncertainty of the ICPT System," *IEEE Trans. Ind. Electron.*, Vol. 60, No. 1, pp. 291–300, Jan. 2013.

[3] M. Pinuela, D. C. Yates, S. Lucyszyn, and P. D. Mitcheson, "Maximizing DC-to-Load Efficiency for Inductive Power Transfer," *IEEE Trans. Power Electron.*, Vol. 28, No. 5, pp. 2437-2447, May 2013.

[4] Z.-H. Wang, Y.-P. Li, Y. Sun, and C.-S. Tang, "Load Detection Model of Voltage-Fed Inductive Power Transfer System," *IEEE Trans. Power Electron.*, Vol. 28, No. 11, pp. 5233-5243, Nov. 2013.

[5] A. P. Hu, "*Selected resonant converters for IPT power supplies*," Ph.D. dissertation, Univ. Auckland, Auckland, NZ, 2001.

[6] S. Lee, B. Choi, and C. T. Rim, "Dynamics Characterization of the Inductive Power Transfer System for Online Electric Vehicles by Laplace Phasor Transform," *IEEE Trans. Power Electron*., Vol. 28, No. 12, pp. 5902-5909, Dec. 2013.

[7] W. Zhang, S.-C. Wong, C. K. Tse, and Q. H. Chen, "Design for Efficiency Optimization and Voltage Controllability of SeriesSeries Compensated Inductive Power Transfer Systems," *IEEE Trans. Power Electron*., Vol. 29, No. 1, pp. 191-200, Jan. 2014.

[8] H. Hao, G. A. Covic, and J. T. Boys, "A Parallel Topology for Inductive Power Transfer Power Supplies," *IEEE Trans. Power Electron*., Vol. 29, No.3, pp. 1140-1151, Mar. 2014.

[9] M. J. Neath, A. K. Swain, U. K. Madawala, and D. J. Thrimawithana, "An Optimal PID Controller for a Bidirectional Inductive Power Transfer System Using Multi objective Genetic Algorithm," *IEEE Trans. Power Electron*., Vol. 29, No. 3, pp. 1523-1531, Mar. 2014.

[10] G. B. Joun and B. H. Cho, "An energy transmission system for an artificial heart using leakage inductance compensation of transcutaneous transformer," *IEEE Trans. Power Electron*., Vol. 13, No. 6, pp. 1013–1022, Nov. 1998.

[11] S. Hasanzadeh, S. Vaez-Zadeh, and A. H. Isfahani, "Optimization of a contactless power transfer system for electric vehicles," *IEEE Trans. Veh. Technol.*, Vol. 61, No. 8, pp. 3566–3573, Oct. 2012.

[12] G. A. J. Elliot, S. Raabe, G. A. Covic, and J. T. Boys, "Multiphase pickups for large lateral tolerance contactless power-transfer systems," *IEEE Trans. Ind. Electron*., Vol. 57, No. 5, pp. 1590–1598, May 2010.

[13] J. Huh, S. W. Lee, W. Y. Lee, G. H. Cho, and C. T. Rim, "Narrow-width inductive power transfer system for online electrical vehicles," *IEEE Trans. Power Electron.*, Vol. 26, No. 12, pp. 3666–3679, Dec. 2011.

[14] B. Song, J. Shin, S. Lee, and S. Shin, "Design of a high power transfer pickup for on-line electric vehicle (OLEV)," in *IEEE International Electric Vehicle Conferrence(IEVC)*, pp. 1–4. Mar. 2012.

[15] K. D. Papastergiou and D. E. Macpherson,"An airborne radar power supply with contactless transfer of energy-part-I: Rotating transformer," *IEEE Trans. Ind. Electron.,* Vol. 54, No. 5, pp. 2874–2884, Oct. 2007.

[16] S. Chopra and P. Bauer, "Driving range extension of EV with on-road contactless power transfer—A case study," *IEEE Trans. Ind. Electron.*, Vol. 60, No. 1, pp. 329–338, Jan. 2013.

[17] G. A. Covic, G. Elliott, O. H. Stielau, R. M. Green, and J. T. Boys, "The design of a contact-less energy transfer system for a people mover system," in *Proc. International Conference on Power System Technology*, Vol. 1, pp. 79–84, 2000.

[18] H. R. Rahnamaee, D. J. Thrimawithana, and U. K. Madawala, "MOSFET based Multilevel converter for IPT systems," In *International Conference on Industrial Technology(ICIT),* pp. 295-300. Feb./Mar. 2014.

[19] H. R. Rahnamaee, U. K. Madawala, and D. J. Thrimawithana, "A multi-level converter for high power-high frequency IPT systems," in *IEEE 5th International Symposium on Power Electronics for Distributed Generation Systems(PEDG),* pp. 1-6. Jun. 2014.

[20] B. X. Nguyen, D. M. Vilathgamuwa, G. Foo, A. Ong, P. K. Sampath, and U. K. Madawala, "Cascaded multilevel converter based bidirectional inductive power transfer (BIPT) system," in *International Power Electronics Conference(IPEC),* pp. 2722-2728. May 2014.

[21] C. Carretero, O. Lucía, J. Acero and J. M. Burdío, "Phase-shift control of dual half-bridge inverter feeding coupled loads for induction heating purposes," *Electronics Letters,* Vol. 47, No. 11, pp. 670-671, May 2011.

[22] C. Carretero, O. Lucía, J. Acero, and J. M. Burdío, "Computational modeling of two partly coupled coils supplied by a double half-bridge resonant inverter for induction heating appliances," *IEEE Trans. Ind. Electron*., Vol. 60, No. 8, pp. 3092-3105, Aug. 2013.

[23] O. Lucía, C. Carretero, J. M. Burdío, and F. Almazan, "Multiple-output resonant matrix converter for multiple induction heaters," *IEEE Trans. Ind. Appl.,* Vol. 48, No. 4, pp. 1387-1396, Jul./Aug. 2012.

[24] C. Carretero, O. Lucía, J. Acero, and J. M. Burdío, "FEA tool based model of partly coupled coils used in domestic induction cookers," *37th Annual Conference on IEEE Industrial Electronics Society.* pp. 2533-2538, Nov. 2011.

[25] A. J. Aronson, "*Vacuum coating system with induction heating vaporizing crucibles*," U.S. Patent 3 657 506, Apr. 18, 1972.

[26] H. P. Ngoc, H. Fujita, K. Ozaki, and N. Uchida, "Phase angle control of high-frequency resonant currents in a multiple inverter system for zone-control induction heating," *IEEE Trans. Power Electron.,* Vol. 26, No. 11, pp. 3357-3366, Nov. 2011.

[27] R. W. Erickson and D. Maksimovic, "*Fundamentals of power electronics*," Springer, 2001.

Yong Li was born in Chongqing, China, in 1990. He received his B.S. degree in Electrical Engineering and Automation from Southwest Jiaotong University (SWJTU), Chengdu, China, in 2013, where he is presently working towards his Ph.D. degree in the School of Electrical Engineering. His current research interests include wireless power transfer, and modular multilevel converters supplying IPT systems for high power applications.

Ruikun Mai was born in Guangdong, China, in 1980. He received his B.S. and Ph.D. degrees from the School of Electrical Engineering, Southwest Jiaotong University (SWJTU), Chengdu, China, in 2004 and 2010, respectively. He was with AREVA T&D U.K. Ltd., London, England, UK, from 2007 to 2009. He was a Research Associate at The Hong Kong Polytechnic University, Hung Hom, Hong Kong, from 2010 to 2012. He is presently an Associate Professor in the School of Electrical Engineering, Southwest Jiaotong University. His current research interests include wireless power transfer and its application in railway systems, power system stability and control, and phasor estimator algorithms and their application to PMUs.

Liwen Lu was born in Jiangsu, China, in 1990. He received his B.S. degree in Electronics and Information Engineering from Southwest Jiaotong University (SWJTU), Chengdu, China, in 2014, where he is presently working towards the M.S. degree. His current research interests include inductive power transfer and power conversion in rail transit applications.

Zhengyou He was born in Sichuan, China, in 1970. He received his B.S. and M.S. degrees in Computational Mechanics from Chongqing University, Chongqing, China, in 1992 and 1995, respectively. He received his Ph.D. degree in Electrical Engineering from Southwest Jiaotong University (SWJTU), Chengdu, China, in 2001. He is presently a Professor at SWJTU. His current research interests include signal processing and information theory applied to power systems, and the application of wavelet transforms to power systems.